Estimating The Bandlimits Of An Unknown Sensor

*Ali Alsam and Graham Finlayson**
The Norwegian Color Research Laboratory
Dept of Computer Science and Media Technology
Gjøvik University College
**University of East Anglia UEA*
Dept of Computer Science

Abstract

Solving for a camera's sensors based on its response to the surfaces of a calibration target is an ill-conditioned problem with an infinite number of possible solutions. To obtain a stable estimate we need to control the solution space by constraining the sensors to match some known physical characteristics e.g. sensors are normally constrained to be positive. The use of constraints limits the uncertainty encountered in sensor recovery and results in improved estimates. Unfortunately, it is not possible to know which exact constraints should be used in recovering an unknown sensor. In this paper we present a method to estimate the support (the region where the sensor's sensitivity is not zero) of a sensor prior to recovering it. If the sensor's support is limited this constraint is very stringent and imposing it on the solution space results in a clear reduction in the uncertainty encountered in the solution. In the results section we show that it is indeed possible to recover a sensor's bandwidth based on its response to a set of reflectances.

1. Introduction

Camera sensor calibration is the problem of estimating the device's spectral sensitivities from its responses to a number of spectrally different surfaces. Generally, there are two approaches to solving the spectral calibration problem, physical and numerical. The physical approach involves using a monochromater[1], which is a device capable of dividing the input light into monochromatic light-beams of known wavelength. By measuring the camera's responses to these light-beams it is possible to achieve an accurate estimate of the spectral sensitivities at each wavelength. Unfortunately, this technique is expensive (a monochromater is both costly to buy and time consuming to use) and as such is limited to well equipped laboratories.

The numerical approach involves solving a linear system of the form:

$$\underline{b}_i = A\underline{x}_i + \underline{\epsilon}_i \quad (1)$$

where A is a $m \times n$ matrix of measured spectra, $\underline{x}_i$ is a $n \times 1$ vector whose elements are the spectral sensitivity at channel i, $\underline{b}_i$ is the camera's response and $\underline{\epsilon}_i$ is the acquisition noise vector. Finally, n is the dimensionality of the data governed by the sampling rate, and m is the number of surfaces.

The goodness of the solution for the spectral sensitivities based on Equation (1) depends on two main factors; the first is the noise level in the response data, and the second is the statistical properties of the spectral data available from the calibration chart.

From linear algebra we know that when solving a linear system of equations with n unknowns such as the system in Equation (1), exactly n equations are needed. Moreover, for a unique solution to exists all n equations need to be linearly independent, i.e. no equation can be estimated as a linear sum of the other equations[2]. Statistical studies based on large data sets clearly indicate that the number of basis functions needed to adequately represent spectral data is limited[3–5]. In other words the actual dimensionality of the data available in matrix A is less or much less than n.

In the parlance of regularization theory[6], a linear system with fewer independent equations than unknowns is referred to as ill-conditioned or rank-deficient[7]. Such systems have an infinite number of solutions, i.e. in the case of sensor recovery as depicted in Equation (1) there are more than one solution $\underline{x}_i$ each of which are equally likely to be the actual device's sensitivities. Indeed, the authors in[8] presented an algorithm to recover the set of all *feasible sensors*, which satisfy certain physical constraints. The findings in[8] indicate that the uncertainty surrounding spectral recovery is proportional to the size of the recovered set, and is governed by a number of factors namely, noise level, the dimensionality of the spectral data, and the constraints imposed on the solution space.

A large body of research in spectral calibration concludes that if the constraints used in the problem formulation reflect the actual properties of the sensor, the estimated

sensitivities will be improved. In [9] the authors constrained the sensors to be positive, smooth, and that they predict the responses within an acceptable noise bound. In [10] the authors added a constraint on the number of peaks allowed in the recovered sensor, while the authors in [11–13] constrained the sensor's magnitude to be small.

Constraints improve upon the recovered sensitivities by restricting the sensor to lie in a smaller region, known as the feasible solution space [14]. The more constraints we add the smaller this region, the more certain we are that the recovered sensor is the actual device's sensitivities. In this paper, we present a new constraint which addresses the special case of sharp or bandlimited sensors, where a sharp sensor is a sensor which is sensitive in a defined region of the visible spectrum. See Figure (1). Sharp sensors

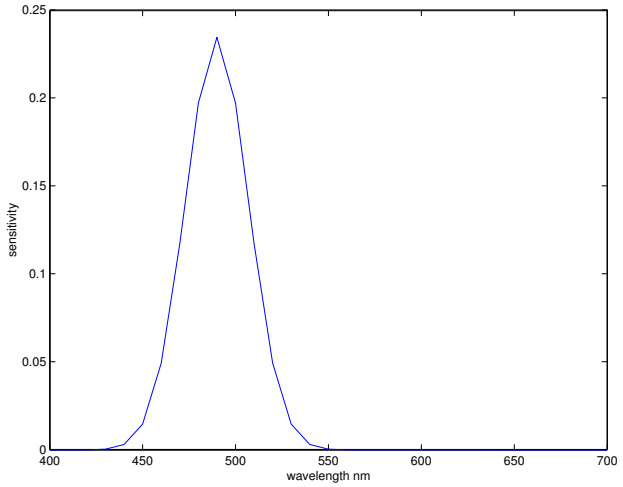

Figure 1: *A sharp sensor which is sensitive only between* 430 *and* $550nm$.

are known to offer a number of advantages over broadband sensors. Finlayson showed that sharp sensors [15] are able to better deal with changes in illumination conditions and hence simplify colour constancy algorithms. Moreover, in the growing field of multispectral imaging [16] sharp sensors are regularly used to sample spectra. To make use of these qualities many ccd sensors are designed to be bandlimited and calibrating them as a special case, with the added bandlimits constraints, is advantageous. This is evident from Figure (1), where we see that using a constraint to restrict the sensor to lie in the wavelength region of $430 - 550nm$ reduces the feasible space to almost one third of $400 - 700nm$.

In [12] it was noted that introducing a constraint which sets the value of the sensitivities to zero in the wavelength region where the sensor is known to be inactive, results in an improved sensor recovery. However, no method is presented by the author to solve for the bandwidth of the sensor. Hence the constraint is not applicable when the actual sensitivities are unknown as is the case when calibrating a device based on measured rgb values and reflectance data. Hence the question addressed in this paper is, given that in real life applications the bandwidth of a sensor is not known, how can we solve for the bandwidth based on the sensor's rgb response to a set of corresponding spectral data? This information is used as a second step to improve upon the recovery of the sensor.

2. Background

For computation, the response of a linear sensor to a spectral stimulus can be modelled as:

$$\underline{p}_i = (E\underline{s})^T \underline{r}_i + \underline{n}_i, \quad i = 1, 2, 3 \tag{2}$$

where E is a diagonal matrix whose diagonal elements are the intensity of the scene's illumination at each discrete wavelength i.e. $E = diag(\underline{e})$, $\underline{s}$ is the surface reflectance, $\underline{r}_i$ is the camera sensitivity vector at channel i, $\underline{n}_i$ is the noise level in the measurement and T is the matrix transpose operator. Spectral functions are normally represented by sampling at 10 nanometer intervals across the visible spectrum [17]. Hence $\underline{e}$, $\underline{s}$ and $\underline{r}$ are 31×1 vectors. Thus,

$$\underline{c} = (E\underline{s}). \tag{3}$$

Based of Equations (2) and (3) we can write the sensor response to a set of m spectral stimuli as:

$$P = C^T R + N \tag{4}$$

where R is a matrix whose columns are the red, green and blue sensitivities of the camera respectively, P is an $m \times 3$ matrix of camera responses and N is a $m \times 3$ measurement noise matrix.

Grouping the response and noise matrices, Equation (4) can be rewritten as:

$$P_N = C^T R \tag{5}$$

where P_N is equal to $P - N$.

In terms of Equation (5) sensor recovery is the problem of estimating R from P_N and C. Numerically, there are two approaches to solving Equation (5), namely direct and iterative methods [18]. Direct methods are those which solve for the spectral sensitivities in one step by inverting Equation (5) for R. Under this approach we include the truncated singular value method also known as the principal eigenvectors [9] and Tikhonov regularization [11–13]. On the other hand, iterative methods search for a solution to Equation (5) which satisfies a number of constraints. In the literature various iterative methods have been used to solve the spectral calibration problem, those include projection

onto convex sets **POCS**[9], quadratic programming[10] and linear programming[19]. These methods are also known as constrained optimization techniques.

The algorithm presented in this paper as well as the mathematical reasoning behind it derives from the fact that given the right constraints, constrained optimization is more robust than the direct methods or unconstrained optimization[12]. This is because the uncertainty in the solution[8] defined by the feasible solution space is reduced. Using an additional constraint to define the bandwidth of the sensors is guaranteed to either improve upon the recovery of the sensor or result in an equally good estimate as the one achieved without imposing the constraint.

3. The Importance of Locality

In this section we explore the importance of the locality imposed by the additional constraint from a statistical regression point of view. Let us assume that we are trying to solve for the best linear model to describe the relation between two data variables x, y, which have the distribution shown in Figure (2a). The best linear fit for the data

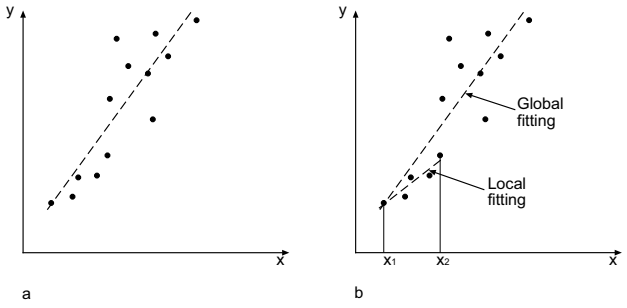

Figure 2: *Global verses local fitting.*

points shown in Figure (2 a) results in the line plotted in the same figure. If we were interested in fitting a linear model based on the same data set but in the limited interval of $x_1 - x_2$ we needn't include the remaining measurement in the regression. In Figure (2 b) we see that defining the regression limits to be between $x_1 - x_2$, results in a line that has a significantly different slope to that of the global line.

The idea of restricting the regression to local limits is analogous to **LOWESS** (Locally Weighted Scatterplot Smoother) due to[20]. **LOWESS** uses weighted regression to fit the first few points defined by a local bandlimit with a little piece of line, and then moves on to the next few points with another piece of line and so on. Local regression is proven to have a number of advantages over classical regression and is known to result in improved model performance[21].

Our bandlimits for the local regression are defined by the window over which the red, green and blue sensors are active. Hence, the locality in recovering a bandlimited sensor refers to the dimensions we use in the regression as oppose to sub intervals along a single dimension as in the example given in Figure (2 b). Knowing the bandlimits, we would expect that fitting the data locally will result in an improved spectral sensitivities solution.

4. Estimating Response from Spectral

In the literature there are many methods[22–24] aimed at solving for a reduced set of basis functions or spectral reflectances to represent a larger set. In essence, the argument behind all the methods is that a limited number of reflectances or colour signals can be used to sufficiently describe a much larger collection of surfaces.

Let us start with a $n \times 1$ colour signal $\underline{c}^T$. We can write $\underline{c}^T$ as a linear combination of a set of basis functions B:

$$\underline{c}^T \approx \underline{w}^T B \tag{6}$$

The weights $\underline{w}^T$ in Equation (6) have dimensions of $1 \times k$, where k is the number of basis functions used and B is a $k \times n$ matrix. Equation (6) can easily be extended to a larger set of colour signals C^T as:

$$C^T \approx W^T B \tag{7}$$

C^T has dimensions $m \times n$, where m is the number of surfaces and n is the dimensionality of the data. Note that W^T in Equation (7) is an $m \times k$ matrix.

In (7) B is an arbitrary basis set. However, for reasons that will become clear it is more useful to choose real reflectances for our basis. Hardeberg et al[22] introduced a method for recovering a small set of surfaces which were broadly representative of the set of all reflectances. We use this set here which we denote $\widehat{Q}$. The "hat" tells us that we are referring to a real physical set of reflectances. We can rewrite Equation (7) as:

$$C^T \approx W^T \widehat{Q}^T \tag{8}$$

where $\widehat{Q}^T$ is a $k \times n$ matrix of the most significant reflectances[22]. From Equation (5), we know that

$$\underline{p}_N = C^T \underline{r} \tag{9}$$

For the response associated with the most significant reflectances $\widehat{Q}$, we can write

$$\widehat{\underline{p}}_N = \widehat{Q}^T \underline{r} \tag{10}$$

If we post-multiply both sides of the equality Equation (10) by the weights W defined in Equation (8), we get:

$$W^T \widehat{\underline{p}}_N = W^T \widehat{Q}^T \underline{r} \tag{11}$$

Equation (11) states that the linear weights defined in Equation (6) can be used to transform the response values corresponding to $\widehat{Q}$ into those of the global set, i.e.

$$\underline{p}_N = W^T \underline{\widehat{p}}_N \tag{12}$$

Before we can examine the goodness of the transform in Equation (8) we need to solve for the weights W. From the work in [8,11] we know that the colour signal matrix C^T is ill-conditioned. Hence, to solve for the weights based on Equation (6), we need to regularise the system. Using Tikhonov regularisation [7], we can write the weights as:

$$W^T = C^T \widehat{Q} \left(\widehat{Q}^T \widehat{Q} + \gamma^2 I \right)^{-1} \tag{13}$$

where γ is the regularisation parameter [25].

The mathematical development so far tells us that, in principle we can predict the responses of reflectances by taking linear combinations of the responses of a small representative set (when we take linear combinations of the RGBs we are in effect taking linear combinations of the underlying reflectances). But, how well does this actually work? An evaluation is presented below. Using 20 reflectances vectors to calculate the linear transform W, the spectral sensitivities of the MegaVision camera and the colour formation equation, we synthesised 264 responses corresponding to the Esser calibration chart. From the 20 responses corresponding to the most significant reflectances i.e. $\underline{\widehat{p}}$ and $\widehat{Q}$, we used Equation (12) to predict the remaining $\overline{2}44$ responses. For the actual and predicted responses, we calculated the absolute error defined as:

$$abs = |\underline{p} - W^T \underline{\widehat{p}}| \tag{14}$$

The experiment was repeated with an increasing levels of Gaussian noise $(1\% - 4\%)$. Table (1) shows the resultant mean, median and maximum absolute errors. The results

Absolute error				
noise level	1%	2%	3%	4%
mean	0.94	1.96	2.90	3.82
median	0.94	1.95	2.94	3.84
max	2.25	3.86	5.42	7.64

Table 1: The the mean, median and maximum error for increasing levels of added Gaussian noise.

shown in Table (1) are based on normalised response data where the maximum value was set to 100. It is evident that the mean and median errors are very close to the level of noise added. Hence we might wonder if it is possible to use the property of being able to synthesis responses from spectral data to estimate the bandlimits. This idea forms the crux of the method to find the limits of a sensor sensitivity. If a sensor has sensitivity from 400 to 550 nanometres, then restricting our representative reflectances to this range should ensure that they are as representative as possible (they need only account for spectral variation in a restricted part of the visible spectrum). It follows then that if we begin with representative reflectances measured for the whole spectrum and then restrict the spectral region of interest we should reduce the prediction error. Of course if we move to too small a wavelength region then the error will increase.

5. Solving for the Bandlimits

In this section we show that using the local regression to estimate responses introduced in the previous section, it is possible to solve for the bandlimits by searching for the best regression solution in terms of the weight W?

Let us consider an arbitrary sharp sensor whose first non-zero sensitivity is $R(\lambda_s)$ and whose last is $R(\lambda_e)$. For such a sensor, W is defined as

$$\widehat{W}^T = C^T \widehat{Q} \left(\widehat{Q}^T \widehat{Q} + \gamma^2 I \right)^{-1} : \ \lambda_s \leq \lambda \leq \lambda_e \tag{15}$$

where C and $\widehat{Q}$ are the portion of the colour signal matrix between $\lambda_s \leq \lambda \leq \lambda_e$. Note that, by varying the start λ_s and end λ_e wavelengths of the sensor, we would converge to a different transforms W. The corresponding response calculated as in Equation (12) is different for every transform $\widehat{\sigma}$ in Equation (15). Moreover, the mean absolute error defined in Equation (14) is also different. Thus, if we vary the start and end wavelengths $\lambda_s \leq \lambda \leq \lambda_e$ and calculate the response and associated error level, we should be able to establish if there is a relation between the error level and the actual bandlimits of the sensor. Our experiments based on synthetic data with varying levels of added noise indicate that the level of prediction error between the synthesised responses and the actual over the actual bandwidth of the sensor is either smaller than that achieved globally or equally good. Hence the mean absolute error can be used as a search criterion for the bandlimits of the sensor. A pseudocode for the method is presented in Algorithm (1)

Algorithm (1): Estimating the bandlimits

Input

- *Colour signals C*
- *Response at a given channel $\underline{p}$*
- *The regularization parameter γ*
- *The colour signal basis vectors $\widehat{C}$*
- *define **ER** =very large positive number*

for λ_s equals 400nm to 700nm step 10nm
for λ_e equals 700nm to λ_s step -10nm

calculate

$$\widehat{W}^T = C^T\widehat{C}\left(\widehat{C}^T\widehat{C} + \gamma^2 I\right)^{-1} : \quad \lambda_s \leq \lambda \leq \lambda_e$$

$$error = mean|\underline{p} - \widehat{W}\widehat{\underline{p}}|$$

if and only if error $<$ *ER*
{
Start wavelength $=\lambda_s$*,End wavelength* $=\lambda_e$*,*
update ER=error
}
next λe
next λs

End Algorithm

6. Results

Our experiments were designed to verify two aspects of the method the first being its ability to estimate the actual bandwidth of an unknown sensor, while the second was the usefulness of imposing the additional bandlimits constraint. To examine the first aspect we synthesised a number of Gaussian sensors with increasing bandlimits. See Figure (3). Using these sensors and the spectral data of

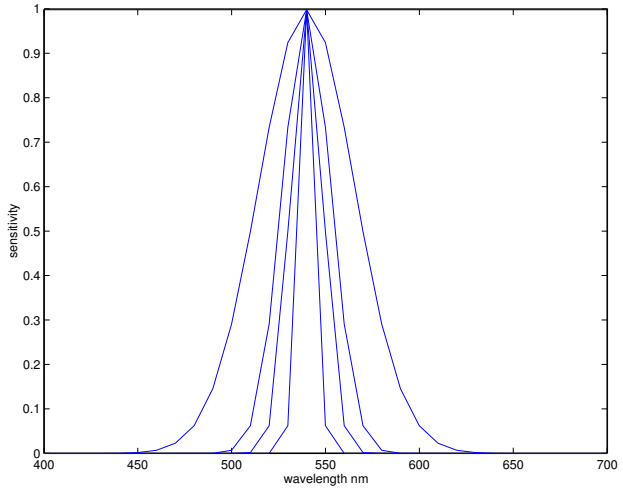

Figure 3: *A number of Gaussian sensors with increasing bandwidth.*

the Esser calibration target we synthesised the sensor's rgb responses. These were then normalized such that the maximum response for all channels was set to 100. We then added 2% Gaussian noise where the maximum noise level at any channel was set to be less than 2. The algorithm's prediction of the start and end wavelengths for a number of bandwidths is tabulated in Table (2). As we see from the data in Table (2) the estimated bandwidth is within $\pm 10nm$ from the actual bandwidth. Knowing that $10nm$ is the sampling rate we can safely say that the recovered bandwidth is in good agreement with the actual width of the sensor. Here we have to note that the goodness of the recovery is subject to the regularisation parameter used. Our experiments show that it is possible to use a much larger regularization parameter to recover the bandwidth than the one derived using the L-curve criterion [25]. Using a regularization parameter of $0.1 - 1$ resulted in acceptable bandwidth estimates.

Actual Start wavelength	Actual End Wavelength	Estimated Start Wavelength	Estimated End Wavelength
540	540	540	540
530	550	530	550
510	570	510	560
490	580	500	570
480	600	490	590
470	610	480	600
440	650	450	640

Table 2: *The actual and estimated start and end wavelengths for a number of Gaussian sensors.*

To test the usefulness of the added constraint in recovering the sensitivities of a real device we estimated the bandwidth of the HP PhotoSmart 912 camera based on its responses to the surfaces of the Esser calibration target. The estimated bandwidths for the blue green and red sensors, were found to be $400 - 540nm$, $430 - 630nm$ and $550 - 700nm$. Using the subsection of spectral data defined by the bandwidth we recovered the sensitivities of the camera using the quadratic programming techniques as described in [10]. Here the recovery was based on 120 patches chosen at random out of the targets 264 surfaces. In keeping with statistical tests conventions we call the 120 set the training set and the remaining 144 the test set.

Using the recovered sensitivities we calculate the relative error at each channel defined as:

$$RE = \frac{abs(p_{es} - p_{ac})}{p_{ac}} \times 100, \tag{16}$$

where p_{es} is the estimated response for the i*th* surface and p_{ac} is the actual response. Further, to asses the goodness of the recovery over all channels we made use of the Euclidian distance defined as:

$$ED = \sqrt{\left(p^r_{es} - p^r_{ac}\right)^2 + \left(p^g_{es} - p^g_{ac}\right)^2 + \left(p^b_{es} - p^b_{ac}\right)^2} \tag{17}$$

where p^r_{es}, p^g_{es} and p^b_{es} and the estimated responses for the red, green and blue channels respectively and p^r_{ac}, p^g_{ac} and p^b_{ac} are the corresponding actual responses. The results for the two error metrics based on the test set (144 surfaces) are shown in Table (3). Knowing that all the responses were normalized such that the maximum value at

relative error			
channel			
mean	3.72	3.41	3.31
median	2.78	2.61	2.36
max	28.61	28.10	28.07
ED error			
	mean	**medina**	**max**
	2.02	1.33	26.77

Table 3: *The mean, median, and maximum relative error at the red, green and blue channels as well as the mean median and maximum Euclidian distance error.*

each channel was set to 100 we find that the mean and median prediction errors for both metrics tabulated in Table (3) are within 2 units, which is likely to be the noise level encountered in the device. Further, by taking two images of the same target under fixed illumination conditions we found that the error levels in Table (3) are equivalent to those achieved by comparing the device's responses for image one and two. Thus, the error levels achieved here are within the devices own variability.

7. Conclusions

In this paper we presented an algorithm to estimate the bandwidth of an unknown sensor from spectral and response measurements. We believe that the added bandwidth knowledge is useful in estimating the spectral sensitivities of bandlimited sensors. This knowledge can easily be incorporated in all the established algorithms for sensor recovery.

References

[1] Bérubé-Lauziére Y. Gingras D. Ferrie F. Color camera characterization with an application to detection under daylight. *Vision Interface Conference 99, Trois-Rivires, Qc*, 1999.

[2] Golub G.H. and Van Loan C.F. Matrix computations. *Baltimore MD: Johns Hopkins University Press*, 1989.

[3] L. T. Maloney and B. A. Wandell. Color constancy: a method for recording surface spectral reflectance. *Journal of the Optical Sociey of America*, pages 29–33, 1986.

[4] Yinlong Sun, F. David Fracchia, and Mark S. Drew. A composite model for representing spectral functions. *A composite model for representing spectral functions*, 1998.

[5] Jon Y. Hardeberg. On the spectral dimensionality of object colors. In *Proceedings of CGIV'2002, First European Conference on Colour in Graphics, Imaging, and Vision*, Poitiers, France, April 2002.

[6] A. Neumaier. Solving ill–conditioned and singular linear systems: a tutorial on regularization. *SIAM Review, 40(3)*, pages 636–666, 1998.

[7] P.C. Hansen. *Rank-Deficient and Discrete Ill-Posed Problems: Numerical Aspects of Linear Inversion*. Siam Monographs on Mathematical Modeling and Computation, 1998.

[8] A. Alsam and G. D. Finlayson. Recovering spectral sensitivities with uncertainty. *In The First European Conference on Color in Graphics, Imaging and Vision*, pages 22–26, 2002.

[9] G. Sharma and H. Trussell. Characterization of scanner sensitivity. *G. Sharma and H. J. Trussell. Characterization of scanner sensitivity. Proc. IS&T/SID Color Imaging Conference*, pages 103–107, 1993.

[10] G. Finlayson, S. Hordley, and Paul Huble. Recovering device sensitivities with quadratic programming. *IS&T/SID Sixth Color Imaging Conference: Color Science, Systems and Applications*, 1998.

[11] Bob Dyas. Robust sensor response characterization. *IS& T/SID Eighth Color Imagining Conference Arizona, USA*, pages 144–148, 2000.

[12] Kobus Barnard and Brian Funt. Camera characterization for color research. *Color Research and Application, Vol. 27, No. 3*, pages 153–164, 2002.

[13] Kobus Barnard and Brian Funt. Camera calibration for colour vision research. *SPIE Conference on Electronic Imaging, Human Vision and Electronic Imaging IV, SPIE Vol. 3644*, pages 576–585, 1999.

[14] V. Chvatal. *Linear Programming*. W. H. Freeman, New York, NY, 1983.

[15] Finlayson G.D., Drew M.S., and B.V. Funt. Spectral sharpening: Sensor transformations for improved color constancy. *JOSA-A*, 11:1553–1563, 1993.

[16] J. Hardeberg, F. Schmitt, H. Brettel, J. Crettez, and H. Matre. Multispectral image acquisition and simulation of illuminant changes. *Colour Imaging: Vision and Technology (L. W. MacDonald and R. Luo, eds.), Wiley*, 1999.

[17] B. Smith C. Spiekermann and R. Sember. Numerical methods for colorimetric calculations: Sampling density requirements. *COLOR research and application*, 17(6):394–401, 1992.

[18] Dimitri P. Bertsekas. *Nonlinear Programming: 2nd Edition*. Athena Scientific, 1999.

[19] F. Koning and P. Herzog. Spectral calibration using linear programming. *In Color imaging, Device Independent Color, Color Hard Copy and Graphics Art V, volume 3963*, pages 36–56, 2000.

[20] W. S. Cleveland. *Elements of Graphing Data*. Wadsworth, Monteray, CA, 1985.

[21] W. Cleveland and C. Loader. Smoothing by local regression: Principles and methods. *Technical Report, AT and T Bell Laboratories, Murray Hill, NY*, 1998.

[22] Jon Yngve Hardeberg, Hans Brettel, and Francis Schmitt. Spectral characterisation of electronic cameras. In *Electronic Imaging*, pages 100–109, 1998.

[23] L. Maloney. Evaluation of linear models of surface spectral reflectance with small numbers of parameters, 1986.

[24] M. Hauta-Kasari, W. Wang, S. Toyooka, J. Parkkinen, and R. Lenz. Unsupervised filtering of munsell spectra. *ACCV (1)*, pages 248–255, 1998.

[25] P.C. Hansen. Analysis of discrete ill-posed problems by means of the l-curve. *SIAM Review*, 34, No. 4:561–580, 1992.